11 WCEE

Published by Elsevier Science Ltd 1996
Paper No.2007. (quote when citing this article)
Eleventh World Conference on Earthquake Engineering
ISBN: 0 08 042822 3

ON THE USE OF ENGINEERING SEISMOLOGY TOOLS IN GROUND SHAKING SCENARIOS

E. FACCIOLI

Department of Structural Engineering, Politecnico di Milano, P.zza L. da Vinci 32, 20133 Milano, Italy

ABSTRACT

The following state-of-art lecture reviews the role and quantitative treatment of some salient physical factors affecting the estimation of the spatial distribution of ground motions, as a basis for constructing damage and loss scenarios for destructive earthquakes. The data obtained, and the effects observed, in the 1994 Northridge and 1995 Kobe earthquakes provide an outstanding motivation for this review. While some factors, notably source-related effects such as rupture directivity, pertain to the domain of seismology, the emphasis is on trying to cast the problem in terms amenable to engineering tools and applications.

KEYWORDS

Arias intensity; Green's functions; ground shaking scenario; non-linear soil response; rupture directivity; shallow soil sites; soil amplification; source effects.

ISSUES INVOLVED

For densely populated areas in seismic regions, damage scenarios and loss estimations for destructive events represent a potentially powerful tool for enhancing the level of earthquake preparedness, and improving disaster prevention policies. Especially for large and complex urban environments, a fundamental prerequisite for such a task is the realistic estimation of the spatial distribution of the ground motion severity generated by the scenario earthquake. The recent cases of the 1994 Northridge and 1995 Kobe (Great Hanshin) events stand out among the destructive earthquakes in recent decades to signal the overwhelming influence that the spatial distribution of ground motions and its close dependence on the source characteristics and the local geological structure can have on the resulting damage.

Two preliminary questions of relevance for the construction of damage scenarios are the choice between deterministic and probabilistic approach, and the type and level of specification of the ground motion. In principle, both deterministic and probability-based scenario earthquakes can be used for representing seismic risk in an area. Probabilistic risk studies that cover all possible damaging events in a region and estimate the cumulative losses from all of them, can help in making an objective pre-selection of the basic features of the scenario earthquake. For instance, it has been suggested that the event that occurs on the seismogenic structure (fault or area source) that contributes most to the risk at the chosen return period, and has the magnitude and location contributing most to the loss be chosen as the scenario earthquake (McGuire, 1995). Starting from this basis, one can then consider the applicability of more or

less complex source, propagation, and site response models depending on the magnitude, the source distance from the zone at risk, the purpose of the loss study, the inventory of objects at risk, and the local geology. Assuming a previous decision has been made as to "where" and "how big" the scenario earthquake will be, in this contribution I will in the main examine briefly some of the physical factors that potentially control the ground shaking scenario in terms of level of severity and spatial distribution. Principal among them are the source geometry and rupture directivity, the treatment of site effects, and the nonlinearity of soil response.

As to the level of specification of the ground motion, it can generally be said that the higher the damage state, the greater the need for more detailed ground motion information. Risk scenarios do not usually approach the task of damage prediction at the structure-by-structure level, that may require the knowledge of the full time history, but make use of some surrogates of it such as peak acceleration or the response spectral ordinates (related to global strength demand), or even the macroseismic intensity. Close to the seismic source, however, different descriptors of the ground motion may be necessary. Some peculiar damage features observed in Northridge and Kobe, especially for steel structures, have been linked to the distinct large-amplitude velocity pulses occurring in the near field. Because it has been found that the response spectrum cannot properly account for the destructiveness of these motions, a new measure of damage potential has been proposed, in the form of the drift demand spectrum (Iwan, 1994). This is calculated from the response of a continuous equivalent shear beam, and is related to the internal, interstory drift demand. On the other hand, integral measures of the ground motion severity, such as the Arias intensity, appear to be more suitable indicators of potential "damage" than the peak values when permanent ground deformations, including slope failures, are involved.

While Northridge and Kobe produced invaluable lessons for all those involved with earthquake issues, many earthquake-prone areas of the world do not share the seismogenic features prevailing in California and Japan and application of methods developed therein to quantify the ground motion hazard may not be appropriate in other seismotectonic contexts. As an example, the seismicity of several zones in the Mediterranean region is governed by faults that seldom generate co-seismic surface ruptures, and whose geometry is ill-defined. It is consequently difficult to associate a scenario earthquake in such zones to a precisely defined tectonic lineament, as commonly made in much of California and Japan. This aspect, as well as the need to construct ground motion estimations with tools basically accessible also to engineers, supports the use of simple methods, such as those based on empirical relations for strong ground motion parameters suitably modified for special conditions, as suggested in the following.

SOURCE-RELATED FACTORS

Representation of the source geometry.

In engineering applications, the spatial distribution of ground motions generated by a seismic source of known location and strength is typically estimated by means of empirical attenuation relations for parameters such as peak acceleration, velocity, or the response spectral ordinates. If the motions are to be assessed in the epicentral area of events of magnitude indicatively larger than 5.5 to 6.0, the point source assumption ought to be normally replaced by a finite source representation, and a consistent definition of source-to-station distance be adopted. An example is presented in Figs. 1 and 2 for the M6.8, 1980 Irpinia earthquake in Southern Italy, where most of the recorded peak horizontal accelerations can be compared to those estimated through a standard attenuation relation (Sabetta and Pugliese, 1987, whose data sample includes the Irpinia records) for rock and stiff soil conditions, actually prevailing at the accelerograph sites. Whereas the point source assumption results in underestimation of the closest observations (Fig. 1), introducing a simplified surface projection of the ruptured area derived from the aftershock distribution and observed surface faulting, leads to a better overall agreement with the data (Fig.2). Nevertheless, the improvement is not large, except for station STU (located on very stiff ground), where the effects of source directivity were probably significant. Note that for the earthquake in question none of the recordings was obtained really close to the source.

The problem is, of course, that if a finite source is to be introduced for predicting the effects of future earthquakes, its geometry must be assumed a priori and this can prove especially difficult in the case of blind faults. One approach is to use empirical relationships among magnitude and different geometric source parameters (e. g. Wells

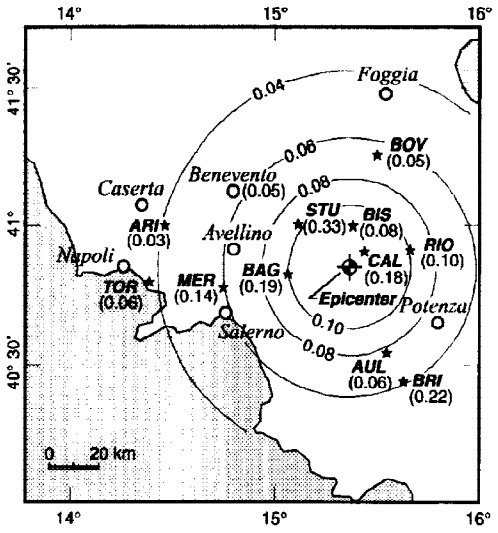

Fig. 1. 1980 Irpinia (Southern Italy) earthquake: peak acceleration contours (in g) calculated with point source and accelerograph locations (asterisks) with recorded values.

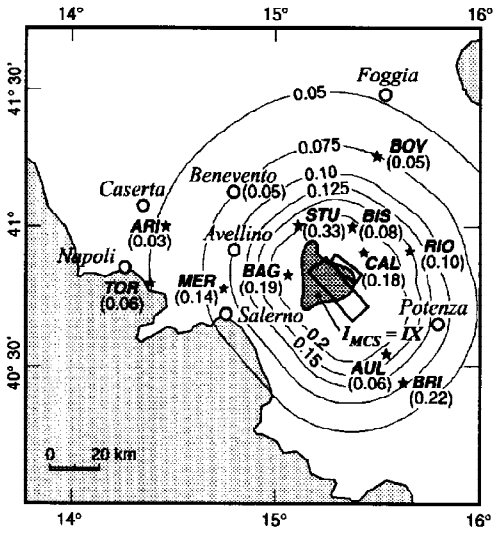

Fig. 2. Same as Fig. 1, but contours calculated with finite source (rectangles).

and Coppersmith, 1994). In countries with a long and well documented historical seismicity record, one can also also rely on intensity maps of the strongest earthquakes in the region. In the previous example of the 1980 Irpinia event, the intensity IX (MCS) isoseism is a reasonably good indicator of the size and position of the ruptured area, see Fig. 2, and also suggests rupture directivity effects to the NW, well in agreement with the relatively high acceleration value at STU station. I illustrate below another possibility, perhaps more attractive for applications, that consists of making some modification to the "circular" attenuation relations to approximately account for primary effects of source finiteness, such as directivity, while retaining the simplicity of the point source representation.

Non-empirical predictions based on realistic source representations (including finite dimensions, simulation of rupture propagation, etc.) can be performed using a variety of seismological models that, however, are in general not directly available to engineering practice. Their use is especially important to quantify the uncertainties in the prediction of the spatial distribution of ground shaking, and their relation to the physical parameters of source and propagation path. Because of computational burden, these calculations are typically limited to frequencies below ~1 Hz, which leaves out a vast range of primary interest for engineering structures. High-frequency approximations, such as those using ray theory and far-field analytical Green's functions (Spudich and Frazer, 1984), can be combined with randomly generated models of the rupture process on the fault to both overcome the previous frequency band limitation and to estimate the uncertainty attached to the ground motion prediction through a large number of simulations (Zollo A., 1995, written communication). When recordings of small earhquakes are available, use of the empirical Green's functions method is obviously attractive. When the geometry and location of the source of the large earthquake are difficult to estimate, schemes of random summation of the Green's functions should be considered, as discussed in the site effects section below.

Directivity.

The damage distribution occurring in the near-source region of a strong earthquake may dramatically depend on the energy-focusing effects produced by the directivity of rupture on the causative fault. In the Northridge earthquake the rupture propagated in the updip direction of an inverse fault, and because of the position of such fault with respect to the dense urban regions, this is likely to have greatly lessened the damage. As a result of directivity, the area above the updip edge of the fault experienced extremely high levels of shaking, notably in velocity (Fig.3). Thus, most of the energy was channeled in the direction opposite from the San Fernando Valley and downtown Los Angeles, where the ground motion severity was greatly reduced and only moderate damage resulted.

The opposite seems to have occurred in the Kobe earthquake, where a dense urban region happened to be located

within a narrow angle from the direction of forward propagation of rupture in the source portion NE of the epicenter (Fig.4). In addition, similar to previous earthquakes in California and elsewhere, the amplitude of motion in the fault-normal direction was observed to be substantially higher than in the fault-parallel direction (Fig. 5). All the main railway and highway routes in the Kobe area, as well as a large portion of the port quaywalls are oriented roughly parallel to to the strike of the seismogenic fault, so that they experienced a very severe out-of-plane motion which may be one of the reasons of the high failure rate of viaducts and bridges. A detailed survey of the permanent seaward displacements suffered by caisson quaywalls has in fact shown that those oriented perpendicular to the fault-normal component of motion experienced substantially larger displacements (Miyata, oral communication, 1996).

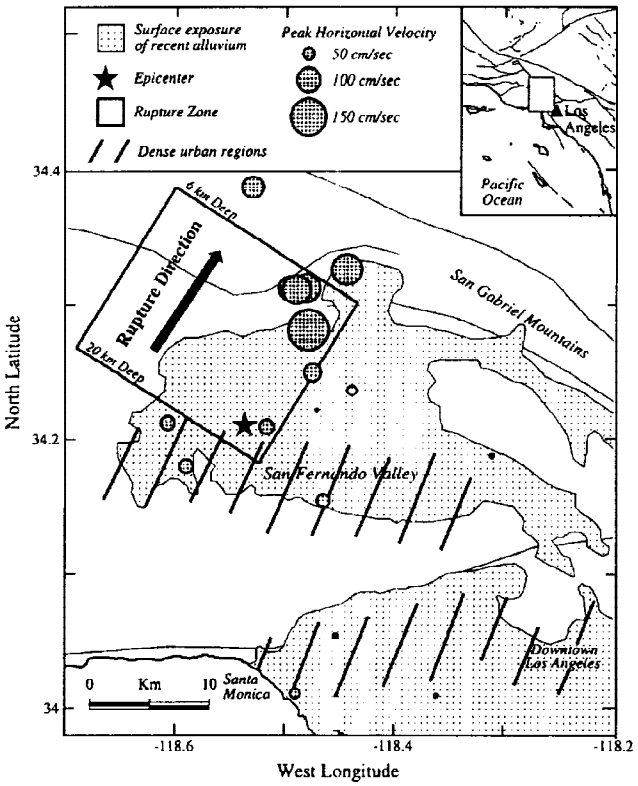

Fig. 3. Epicenter, surface projection of fault rupture, dense urban regions, and average peak ground velocities recorded from the Mw 6.7, 1994 Northridge earthquake. From Somerville (1996).

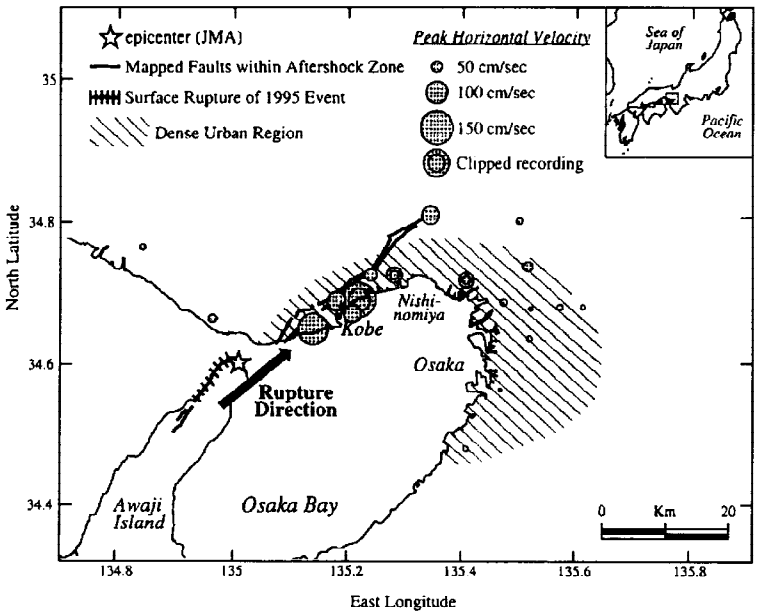

Fig. 4. Epicenter, mapped active faults within the aftershock zone, dense urban region, and average peak velocities recorded from the Mw 6.9, 1995 Kobe earthquake. From Somerville (1996).

It has been very recently shown on the basis of a representative sample of observations (including Loma Prieta, Northridge, Kobe) that, for near-fault conditions, the influence of forward rupture directivity, and notably the difference associated with the fault-normal component of motion, becomes large in the period range beyond about 0.5 sec and increases with increasing period. The distance range of interest varies between few km for M_w 6.0, to 20 km or so for M_w 7.5. It is also reassuring that the effect in question can be realistically handled at the level of empirical prediction of the response spectral ordinates, by increasing by an overall factor of two in the worst case (fault-normal component under forward directivity conditions) the predicted median value in average near-field conditions for periods larger than 0.5 sec (Somerville, 1996). This also gives an indication as to how such a class of near-source effects can be accomodated in forthcoming code provisions for design earthquakes.

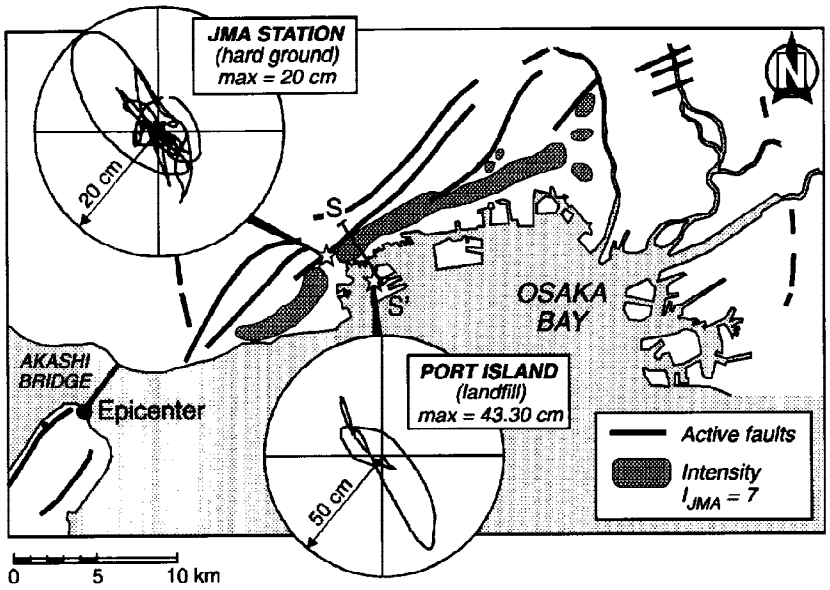

Fig. 5. Orbits of horizontal particle displacement showing predominance of the fault-normal component of motion at Kobe JMA and Port Island stations.

Because the response spectrum is rather insensitive to the significant duration of ground motions, it is of interest to predict the influence of directivity on alternative indicators of the severity of shaking, such as the Arias intensity Ia, that more closely reflect the influence of duration and, due to this reason, have been shown to be well correlated to geological damage, e. g. slope failures (Wilson and Keefer, 1985), and permanent ground settlements (Faccioli et al., 1996b). A theoretically derived attenuation relation for Ia (as well as for the analogous cumulative measures of ground velocity and displacement) that accounts for directivity, was proposed some years ago with parameters calibrated on strong motion data from the Mediterranean region (Faccioli, 1983). This basically applies for a point source and for horizontal motion has the form

$$\log I_a = 1.065 M_w - 2 \log R + \log D_a(\theta) - 4.63 \qquad (1)$$

where I_a is in m/s, and R (hypocentral distance in km) is limited within the 10 to 50 km range. Source directivity is described by the function

$$D_a(\theta) = \frac{3 - m\cos\theta}{(1 - m\cos\theta)(2 - m\cos\theta)^2} \qquad (2)$$

where θ is the angle between the direction of source rupture propagation and the hypocentre-to-receiver direction, and m (< 1) is the ratio between the rupture propagation and the S-wave propagation speeds, generally assumed between 0.7 and 0.85. The effects of directivity are best taken into account by the previous expression in the case of nearly vertical faults (strike-slip and dip-slip) and rupture propagation along the strike of the fault. These conditions are approximately verified for the previouly considered Irpinia earthquake, which had a normal mechanism on a fault steeply inclined (~70°) to the NE. Although the rupture was bilateral, most of the energy was radiated in the NW direction and only this contribution is considered here for simplicity. Fig. 6 illustrates both the I_a contour lines calculated with (1) and (2) for M_w 6.8, $m = 0.8$, and the values observed at the closest accelerograph stations within ± 90° of the direction of rupture propagation (note that Da (180°) = 0.27, while Fig. 6 may erroneously suggest a

vanishing value). The reasonable agreement for the STU, CAL, and MER stations appears to confirm that the effects of directivity were indeed appreciable for this earthquake. This example, and those illustrated in a previous study (Faccioli, cit.) suggest that introducing an elementary description of the rupture characteristics can significantly improve the prediction capability of attenuation relations for important categories of seismogenic faults.

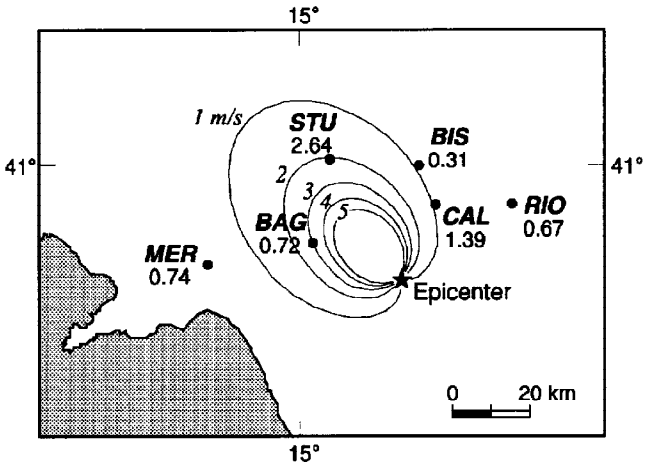

Fig. 6. Observed Arias intensities in the NW half of the 1980 Irpinia earthquake epicentral region, in m/s, and corresponding contours calculated by Eqs. (1) and (2) showing probable directivity effects.

SITE EFFECTS

Modelling and role of local geological structure. The role played by the surface geology on the spatial distribution of earthquake effects has probably been crucial in Kobe, where the heaviest damage was concentrated in a narrow zone, referred to in Japanese media as "disaster belt", extending from Awaji Island through Kobe City and to the north of Osaka prefecture (Fig. 5). The intensity inside this belt was the highest, i. e.VII, in the Japanese JMA scale. The small number of near-field acceleration recordings obtained for the main shock (see also Fig. 4), and the unsuitable location of the stations, does not allow to establish a direct association between the damage distribution and the local ground response on the basis of instrumental observations (Pitarka et al., 1996). Also, since the damage concentration is closely related to the structural features of the affected buildings, a tradeoff undoubtedly exists between the ground shaking and the structural aspects.

The combined influence of the local geological structure within few km depth, and of the soft near surface sediments, was investigated by Pitarka et al. (cit.) and Kawase (1996) using both 2D and 1D models of geological cross-sections transversal to the damage belt. The location of the 4 km long × 1 km deep cross-section S-S' used by Kawase is shown in Fig. 5, while the cross-section studied by Pitarka et al. lies some 5 km to the E and has dimensions of 3 km × 2 km. The latter authors base their work on successful modelling of the motions from an aftershock recorded by a temporary instrumental array located across the central part of the damage belt, in the 0.1-3.0 Hz frequency range. On the other hand, Kawase, who uses as an input to his 2D model a waveform obtained from the deconvolution of the Kobe JMA stiff site recording, proves the reliability of his simulations by reproducing rather satisfactorily the surface records at the Port Island (Fig. 5) and Port Office accelerograph sites, both located in correspondence to the analysed cross-section. Based on deep reflection profiles run after the earthquake, both models share as a key feature a strong lateral contrast in P- and S-wave velocity near their northern boundary, related to a ~1 km vertical offset apparently created in the Pliocene basement by the geological activity of the faults mapped in Fig 5, which has also lead to the creation of the local deep basin structure. This geometry is apt to generate a narrow zone on the surface of the sedimentary deposit, where constructive interference between the upward propagating direct body waves and the horizontally propagating surface waves diffracted by the edge of the basin gives rise to very strong amplification of ground motion. The additional effect of the soft near-surface layers is treated by 1D models excited with the output of the 2D analyses. Of special interest is the calculated surface peak velocity distribution in Fig. 7, showing that in the ~1000 m wide interval corresponding to the belt of heavy damage peak velocities may have reached up to 2 m/s, and that the respective amplication factors with respect to the Osaka formation outcrop at the basin edge have reached values of 3 to 4. Even higher values are calculated by Pitarka et al. in correspondence to the damage belt, while the general pattern is similar. In the southernmost portion of the cross-section the 1D effect controls the response, accounting for an amplication factor of 2.

The principal lesson from this outstanding case history is that for dense urban areas close to sedimentary basins or other strong irregularities in the surface geology, and located in highly seismic zones, priority in eartquake risk

prevention activities should also be given to determining the crustal geometry and velocity models at depth ranges that may extend from several hundreds of m to a few km, since these are likely to have a profound influence on the earthquake ground shaking. If realistic models become available for the surface geologic structures, there appears to be no lack of computational tools for reproducing seismic site effects in most of their salient aspects.

Simplified methods and inherent uncertainties.
A simplified treatment of the influence of the near-surface geology can be included in ground motion scenarios through a combination of empirical relations and digital geologic maps, that can be conveniently implemented by a GIS.
Several attenuation relations segregate the local site conditions in few broad classes, and this elementary classification can be applied to transform the available geologic maps into a "site" information layer required for the application of the GIS. As an example, the attenuation relation used to construct the acceleration contours in Fig.2 has the form (Sabetta and Pugliese, cit.)

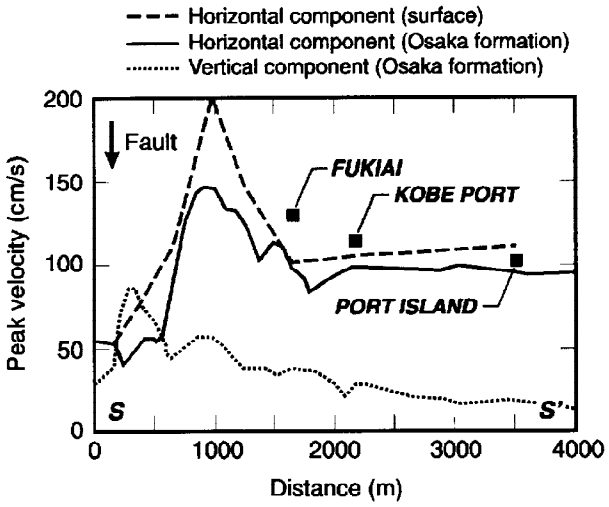

Fig. 7. Peak velocities across concentrated damage belt in Kobe calculated by Kawase (1996) along cross-section S-S' shown in Fig. 5. "Osaka formation" curves are from 2D linear analysis , while the "surface" curve also accounts for nonlinear response of surface soil layers. Solid symbols denote observed values.

$$\log PHA = -1.562 + 0.306M - \log(R^2 + 5.8^2)^{1/2} + 0.173S \qquad (3)$$

where PHA (g) is the peak horizontal acceleration, M is equivalent to moment magnitude, R (km) is the closest distance to the surface projection of the fault rupture, and S is a site descriptor such that S=0 for both stiff (including rock) and deep soil sites, and S=1 for shallow soil sites. The latter are indicatively defined as having an alluvium thickness between 5m and 20m and an average S-wave velocity v_s between 400 and 800 m/s. It follows that on shallow soil sites PHA is amplified by an estimated average factor of 1.5 with respect to rock and deep soil sites. Note that soft and shallow alluvium sites are essentially missing from the classification.

A different approach underlies a recent empirical relation which quantifies the site effect through a physical parameter, i. e. the average v_s value to a depth of 30 m, and has the form (Boore et al., 1994)

$$\log PHA = -0.19 + 0.216M - 0.777\log(R^2 + 5.48^2)^{1/2} - 0.364\log v_s \qquad (4)$$

where PHA, M and R are defined as before and the average v_s is in m/s. Eq. (4) is based on borehole data from more than 100 sites. Obviously, in the absence of in-situ velocity measurements, the use of (4) requires the use of appropriately calibrated correlations with the characteristics of local geologic materials.

When applying simplified methods, an important problem regards the uncertainty in the predicted ground motion values, notably for those categories of site conditions that are known from previous earthquakes to be prone to strong local amplification, and may therefore suffer high concentration of damage in future earthquakes. To illustrate this point, I choose an example taken from an ongoing research project aimed at the construction of a damage scenario for the city of Catania, in Sicily, which has a present population of about 500000. The selected scenario earthquake is similar to the 1693 event, which had an estimated Ms between 7.0 and 7.5 and caused about 15000 victims out of a total city population of 18000. For the sake of brevity, only peak acceleration is used here to describe the ground motion severity. Displayed in Fig 8 is a hypothetical reconstruction of the geometry of the 1693

source, as well as the epicenter of a moderate earthquake (Mw 5.7) that occurred in December 1990 causing some damage in nearby coastal towns, including Catania. This event was recorded at a number of accelerograph stations including the two shown in the figure. GRR lies some 50 km from the 1990 epicenter on thick lava flows from historic volcanic eruptions of Mt. Etna, and it can be considered representative of the ground conditions prevailing in several older sections of Catania. On the other hand, CAT is a site 30 km from the 1990 epicenter on unconsolidated fluvial deposits with indicative vs values between 120 and 200 m/s in the upper 30 m and underlain by much stiffer clays where values in excess of 600 m/s are reached at about 40 m depth (Maugeri et al., 1988). CAT is representative of site conditions prevailing in the industrial development zone in the Southern part of the city, and in the 1990 earthquake it experienced the highest recorded accelerations, with a peak of 0.24g, and strong evidence of local amplification at a dominant frequency of 5 Hz..

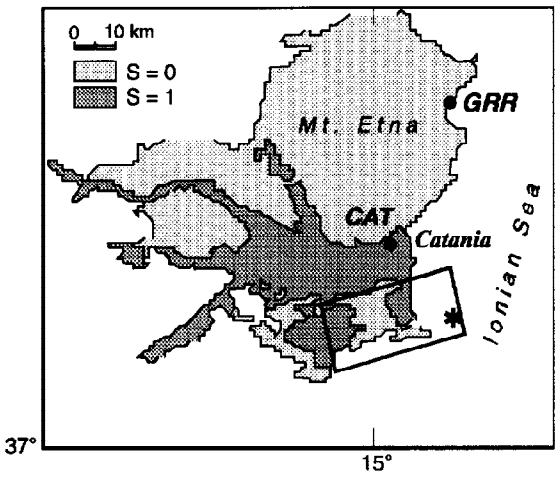

Fig. 8. Portion of Eastern Sicily showing the location of Catania city, the hypothetical surface projection of the rupture area of the 1693 earthquake (large rectangle, after D'Addezio and Valensise, 1991), the epicenter of the December 1990 earthquake (asterisk), and the accelerograph stations CAT (on shallow soft alluvium) and GRR (on lava rock). The zones where predominant site conditions of type S=0 (stiff) or S=1 (shallow soil), see Eq. (3) are shown by different shading.

For a M 7.0 scenario event with a ~10 km shortest source distance, the peak acceleration at the CAT site estimated with (3) would be 0.5 g ±0.24g. If (4) is used instead, with an average v_s = 170 m/s, the estimated PHA value is almost the same. An independent check of the reliability of this estimate can be obtained by using the largest horizontal component (NS) of the 1990 CAT accelerogram, shown in Fig. 9, as an empirical Green's function for the large event, which seems an acceptable assumption in view of the position of its epicenter. A random summation scheme is adopted to synthesise the ground motion for the large event, of which one only needs to specify the stress drop (Ordaz et al., 1995). The extended target area is approximated by a point source, whose rupture duration, however, is in accordance with its dimension. This method was selected in view of the uncertainty on the exact position and dimensions of the 1693 source and of the good results reported for the Mexican earthquakes by Ordaz et al. By taking a target seismic moment corresponding to M 7.0, and a stress drop of 100 bar for both the small and the large events, 22 different synthetic acceleration histories were generated, from which an average peak value of 0.78g is obtained with a standard deviation of 0.15g. Also shown in Fig.9 is one of the synthetic accelerograms that has a peak equal to the sample average. Thus, the independently estimated maximum acceleration is larger than the mean +1σ predicted by the attenuation relation, indicating the large amplification potential in the zones where the site conditions are similar to CAT.

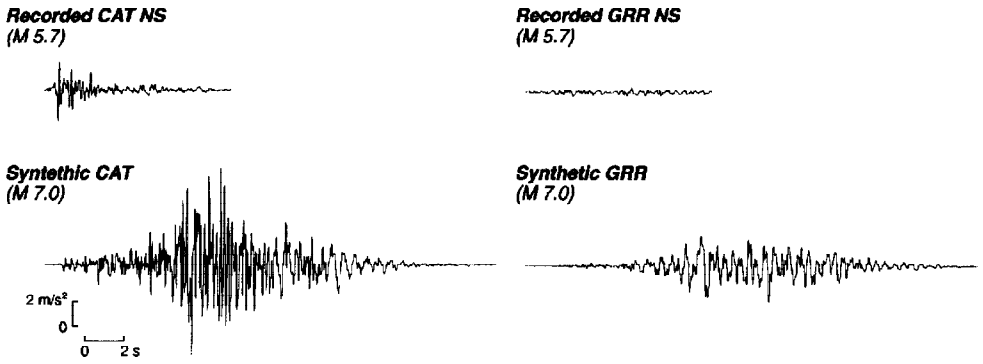

Fig. 9. Empirical Green's functions and synthesised time histories of horizontal acceleration at CAT and GRR. The latter is scaled, to correct for the distance difference with respect to CAT.

To properly evaluate the extent of local amplification at sites like CAT with respect to the stiff ground conditions that prevail in several sections of the city, the previous procedure was applied to the strongest horizontal component of the GRR recording (PGA = 0.04*g*), also shown in Fig. 9. After correcting the synthetics for geometrical spreading in order to have an estimate applicable at the same distance as the CAT site, a peak value of 0.28 ± 0.07*g* is obtained. One simulated time history having a peak equal to the sample average is shown in Fig. 9. The corresponding estimate yielded by (3) is 0.33 ± 0.16*g*, in rather good agreement with that obtained from the synthetics. In conclusion, the present example indicates that the use of empirical relations in constructing ground motion scenarios for potentially destructive earthquakes is likely to provide acceptable estimates for average or stiff site conditions. However, special care should be devoted to the in-situ determination of the geotechnical characteristics of shallow and soft soil sites, as well as of other types of sites known to have anomalous seismic response, so that improved estimates can be obtained by more sophisticated approaches.

Non-linearity of soil response.

Instrumental observations and analyses pertaining to non-linearity aspects of soil response were extensively reviewed in a very recent workshop (Iai, 1996). Hence, I will only briefly consider the evidence contained in the important set of data provided by the Northridge earthquake, mostly representative of the response of consolidated sediments with water table not close to the surface. Data from soft, water-saturated soil sites prone to developing high excess pore pressures and, therefore, also cyclic mobility and liquefaction (of which some remarkable examples were recorded in Kobe) will not be discussed because a site-specific interpretation and analysis are often required.

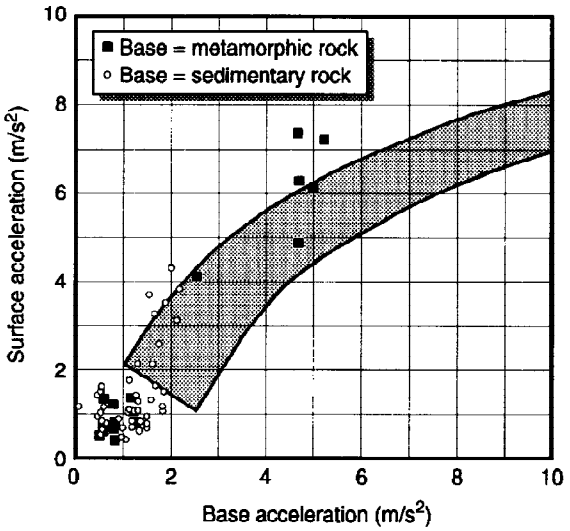

Fig. 10. *Stiff soil sites amplification response in Northridge earthquake (open and solid symbols), and range of 1D numerical simulation results (shaded zone) for deep cohesionless site with ~70% relative density.*

The Northridge data compilation made by Borcherdt (1996) was used to construct the peak horizontal acceleration plot of Fig. 10, which considers only the observed response of stiff soil sites, indicatively defined as having an average vs value between 180 and 360 m/s (or an average NSPT between 15 and 50). The surface peak acceleration at such sites is plotted vs. a "base acceleration" that consists of the peak horizontal value observed either at metamorphic or at sedimentary rock sites located within appropriate distance and azimuth ranges with respect to the epicenter. The observations are compared with a range of numerical results obtained with 1D dynamic finite element simulations that make use of a sophisticated constitutive model with plastic work-hardening, whose parameters are calibrated against cyclic and static test data for a real sand at a relative density of 70% (Faccioli et al., 1996a). The numerical model, which was excited by many different incident signals having the form of real accelerograms, describes a deep cohesionless soil site whose elastic moduli increase with depth in the upper 11m (160 m/s $< v_s <$ 240 m/s) and is underlain by a homogeneous halfspace without intervening impedance contrast. This probably explains the partial lack of agreement between the data (especially those referred to the hardest rock sites) and the simulations results at the higher acceleration levels in Fig. 10. On the other hand, the main indication of Fig. 10 is that only very moderate nonlinearity effects,if any, can be expected up to almost 0.5*g* on deep consolidated sediments such as those found in the Los Angeles and San Fernando Valley areas, and that some salient general features of their seismic response can be captured by simple wave propagation models that must, however , reproduce well the constitutive behaviour of real soils.

SOME CONCLUSIONS

With the aid of some recent observations and a few examples of applications, I have presented an attempt at exploring to what extent some physical factors that are likely to have a strong influence on the spatial distribution of ground motion (source finiteness and rupture directivity, local amplification, soil non-linearity) can be realistically accounted for by simple approaches within the reach of engineering practice. For the source-related aspects the answer is mostly conditioned by the a-priori knowledge of the geometry and orientation of the seismogenic structures, highly uncertain in many populated and highly seismic zones of the world. On the other hand, more than to the development of new models, substantial effort for improving the prediction of site effects in a given area should go into field investigations for determining the near-surface geologic structure and the associated seismic velocity models. This may involve depths ranging from few tens to many hundreds of meters, as dramatically shown by the interpretation of local site effects in Kobe.

ACKNOWLEDGMENTS

I am indebted to Roberto Paolucci and Vera Pessina for analyses and calculations related to some of the examples discussed, and to Stefano Bacci for the figures and graphic presentation. The work presented was supported by Consiglio Nazionale delle Ricerche (Gruppo Nazionale Difesa Terremoti) of Italy, under Contract no. 94.01678.PF54.

REFERENCES

Boore, D., W. Joyner and T. Fumal. Estimation of response spectra and peak accelerations from Western North American Earthquakes. An interim report. Part 2. *U. S. Geological Survey Open-File Report 94-127,* Menlo Park, California.

Borcherdt R. (1996). Preliminary amplification estimates inferred from strong ground motion recordings of the Northridge earthquake of January 17, 1994. *Proc. Intern. Workshop on Site response Subjected to Strong Earthquake Motions*, Jan. 16-17, Yokosuka, Japan

Faccioli E. (1983). Measures of strong ground motion derived from a stochastic source model. *Soil Dynamics Earthq. Engin.*, **2**, 135-149.

Faccioli, E., R. Paolucci and S. Pedretti (1996a). Contribution to the special comparative study on the non-linearity. *Proc. Intern. Workshop on Site response Subjected to Strong Earthquake Motions*, Jan. 16-17, Yokosuka, Japan

Faccioli, E., R. Paolucci and A. Pecker (1996b). Code-oriented studies on the behaviour of shallow foundations under seismic loading. *These Proceedings.*

Iai S., (Editor)(1996). *Proc. Intern. Workshop on Site response Subjected to Strong Earthquake Motions*, Jan. 16-17, Yokosuka, Japan. In press.

Iwan W. (1994). Near-field considerations in specification of seismic design motions for structures. *Proc. 10th European Conf. on Earthq. Engin.*, August 28-September 2, Vienna, Austria, **1**, 257-267.

Kawase H. (1996). Strong motion simulation in Sannomiya, Kobe, during the 1995 Hyogo-ken Nambu earthquake considering nonlinear response of shallow soil layers. *Proc. Intern. Workshop on Site response Subjected to Strong Earthquake Motions*, Jan. 16-17, Yokosuka, Japan

Maugeri, M., A. Carrubba and P. Carrubba (1988). Caratterizzazione dinamica e risposta del terreno nella zona industriale di Catania. *Ingegneria Sismica*, **V**(2), 9-17.

Mc Guire R. (1995). Scenario earthquakes for loss studies based on risk analysis. *Proc. 5th Intern. Conf. on Seismic Zonation.* October 17-19, 1995, Nice, France, **II**, 1325-1333.

Ordaz, M., J. Arboleda and S. K. Singh (1995). A scheme of random summation of an empirical Green's function to estimate ground motions from future large earthquakes. Submitted to *Bull. Seism. Soc. Am.* for publication.

Pitarka, A., K. Irikura and T. Iwata (1996). Was the basin edge geometry responsible for the ground motion amplification in the disaster belt-like zone during January 17, 1995, Kobe (Hyogo-ken Nanbu), Japan earthquake? *Proc. Intern. Workshop on Site response Subjected to Strong Earthquake Motions*, Jan. 16-17, Yokosuka,

Japan
Sabetta, F. and A. Pugliese (1987). Attenuation of peak horizontal acceleration and velocity from Italian strong-motion records. *Bull. Seism. Soc. Am.*, **77**, 1491-1513.
Somerville P. (1996). Forward rupture directivity in the Kobe and Northridge earthquakes, and implications for structural engineering. *Proc. Intern. Workshop on Site response Subjected to Strong Earthquake Motions*, Jan. 16-17, Yokosuka, Japan
Spudich, P. and L. Frazer (1984). Use of ray theory to calculate high-frequency radiation from earthquake sources having spatially variable rupture velocity and stress drop. *Bull. Seism. Soc. Am.*, **73**, 2061-2082.
Wells, D. and K. Coppersmith (1994). New empirical relationships among magnitude, rupture length, rupture width, rupture area, and surface displacement. *Bull. Seism. Soc. Am.*, **84**, 974-1002.
Wilson, R. and D. Keefer (1985). Predicting areal limits of earthquake induced landsliding. In Ziony J. (Ed.): Evaluating earthquake hazards in the Los Angeles region. *U. S. Geological Survey Professional Paper 1360*, 317-493.